

## **Measurement report: Dual-carbon isotopic characterization of carbonaceous aerosol in Beijing and Xi'an: distinctions in primary versus secondary sources**

Haiyan Ni<sup>1,2</sup>, Ru-Jin Huang<sup>1,3</sup>, Max M. Cosijn<sup>2</sup>, Lu Yang<sup>1</sup>, Jie Guo<sup>1</sup>, Junji Cao<sup>1,3</sup>, and Ulrike Dusek<sup>2</sup>

<sup>1</sup>State Key Laboratory of Loess and Quaternary Geology, Center for Excellence in Quaternary Science and Global Change, Key Laboratory of Aerosol Chemistry and Physics, Institute of Earth Environment, Chinese Academy of Sciences, Xi'an, 710061, China

<sup>2</sup>Centre for Isotope Research (CIO), Energy and Sustainability Research Institute Groningen (ESRIG), University of Groningen, Groningen, 9747 AG, the Netherlands

<sup>3</sup>Institute of Global Environmental Change, Xi'an Jiaotong University, Xi'an, 710049, China

*Correspondence:* Ru-Jin Huang (rujin.huang@ieecas.cn)

## S1. Estimation of $r_{bb}$ and $r_{fossil}$

$r_{bb}$  and  $r_{fossil}$  are primary OC/EC ratio for biomass burning and fossil fuel combustion, respectively.  $r_{fossil}$  is the weighted average of  $(POC/EC)_{coal}$  (i.e.,  $r_{coal}$ ), and  $(POC/EC)_{vehicle}$  ( $r_{vehicle}$ ). The weight associated with  $r_{coal}$  (denoted as  $w_{coal}$ ) is the relative contribution of coal combustion to fossil EC. That is,

$$w_{coal} = \frac{EC_{coal}}{EC_{fossil}} = \frac{EC_{coal}}{EC_{coal} + EC_{liq.fossil}} \quad (S1)$$

where  $EC_{fossil}$  is the sum of  $EC_{coal}$  and EC from liquid fossil fuel combustion (i.e., vehicle emissions;  $EC_{liq.fossil}$ ).

Eq. (S1) can be formulated as:

$$w_{coal} = \frac{f_{coal}}{f_{fossil}} = \frac{f_{coal}}{f_{coal} + f_{liq.fossil}} \quad (S2)$$

where  $f_{coal}$  and  $f_{liq.fossil}$  are the relative contribution of coal combustion and liquid fossil fuel combustion to EC, respectively. The sum of  $f_{coal}$  and  $f_{liq.fossil}$  is  $f_{fossil}$  of EC, which is well constrained by  $F^{14}C$  of EC. The PDFs of  $f_{coal}$  and  $f_{liq.fossil}$  (e.g., Fig. S4), derived from the Bayesian calculations detailed in Sect. 2.4 of the main text, are used to calculate the PDFs of  $w_{coal}$ .

Best estimates of  $r_{bb}$  ( $4 \pm 1$ ; average  $\pm$  SD),  $r_{coal}$  ( $2.38 \pm 0.44$ ), and  $r_{vehicle}$  ( $0.85 \pm 0.16$ ) are defined through a literature search as described in Ni et al. (2018), and their values are comparable to values used in earlier studies (Zhang et al., 2014, 2015).

## S2. Uncertainties of $^{14}C$ source apportionment results

To propagate uncertainties, we conducted a Monte Carlo simulation with 10000 individual calculations to propagate experimental uncertainties and uncertainties in parameters (e.g.,  $F^{14}C_{nf}$ ,  $r_{bb}$  and  $r_{fossil}$ ) following Eq. (3–12).

For each calculation,  $F^{14}C$  and mass of EC and OC were randomly chosen from a normal distribution symmetric around the measured values with the experimental uncertainties as standard deviation (SD). For  $F^{14}C_{nf}$ ,  $r_{bb}$ ,  $r_{coal}$  and  $r_{vehicle}$ , random values of each parameter were chosen from a triangular frequency distribution with its maximum frequency at the central value and 0 frequency at the lower limit and upper limit of each parameter. For  $w_{coal}$ , random values from the respective probability density function (PDF) of  $w_{coal}$  were used (Supplement S1). In this way 10000 random sets of variables were generated. For  $f_{bb}(EC)$ ,  $f_{nf}(OC)$ ,  $EC_{bb}$ ,  $EC_{fossil}$ ,  $OC_{nf}$  and  $OC_{fossil}$ , the derived mean represents the best estimate, and the SD represents the combined uncertainties (Table S3). For  $POC_{bb}$ ,  $OC_{o,nf}$ ,  $POC_{fossil}$ ,  $SOC_{fossil}$ ,  $SOC$  and  $f_{fossil}(SOC)$ , the median value is considered as the best estimate and the interquartile ranges (25th–75th percentile) represent the combined uncertainties, because the PDFs of  $POC_{fossil}$  and  $SOC_{fossil}$  are asymmetric (Fig. S5, Table S4). The median values for  $POC_{bb}$  and  $OC_{o,nf}$  are very close to their mean values due to their symmetric PDFs (Fig. S5).

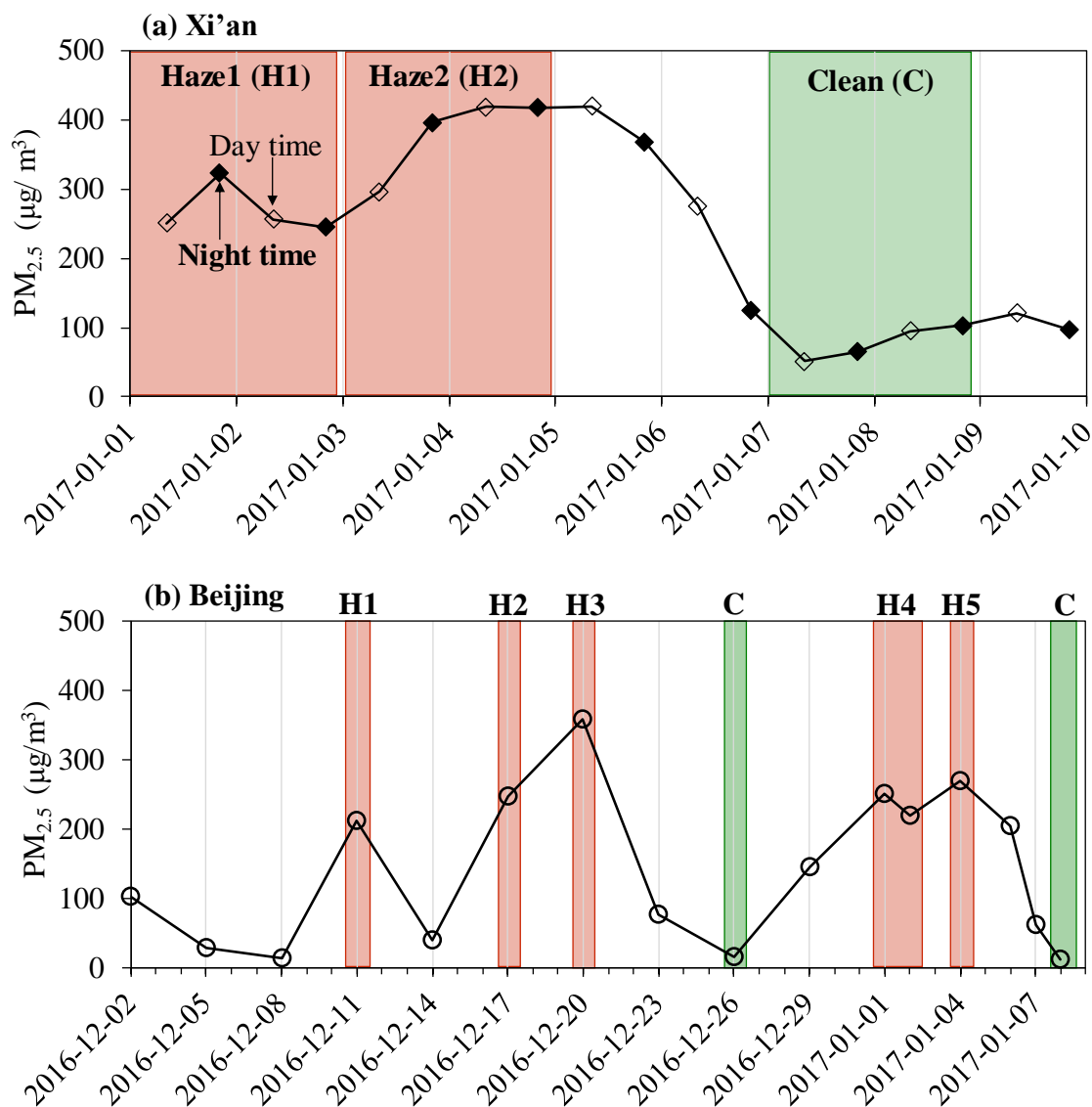


**Figure S1.** PM<sub>2.5</sub> mass concentrations (µg m<sup>-3</sup>) in Xi'an and Beijing during the measurement periods. The dashed areas indicate the selected samples for <sup>14</sup>C analysis. **(a)** 12h averaged PM<sub>2.5</sub> concentrations in Xi'an, the open symbols represent daytime samples, the filled square symbols represent nighttime samples. **(b)** 24h averaged PM<sub>2.5</sub> concentrations in Beijing. Samples selected for <sup>14</sup>C analysis are highlighted in red (indicating haze periods) and green (clean periods). For details, see Table S1.

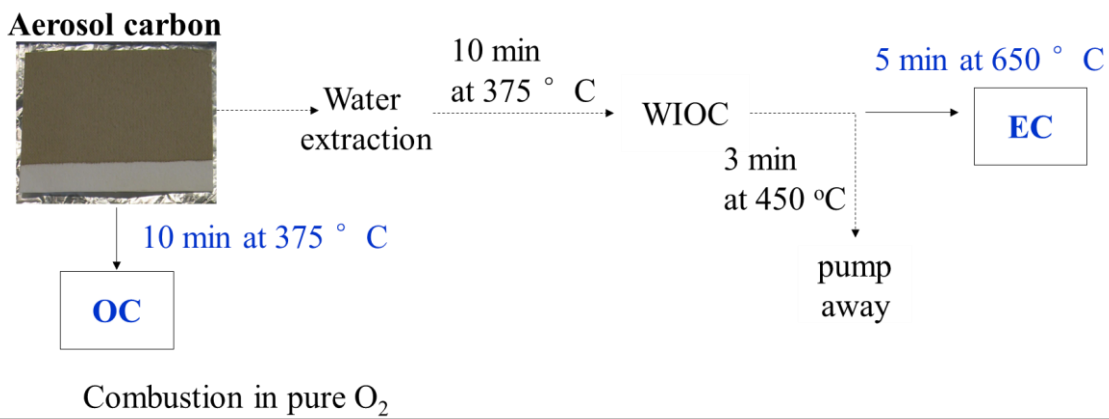


**Figure S2.** Temperature protocol of OC and EC isolation for <sup>14</sup>C measurements was implemented on aerosol combustion system (Dusek et al., 2014) in pure O<sub>2</sub>. OC is extracted by combusting the filter samples at 375 °C for 10 min. To isolate EC, OC is completely removed by 3 steps in order: water-extraction of filter samples (i.e., removal of water-soluble OC), combustion at 375 °C for 10 min (removal of water-insoluble OC; WIOC) in O<sub>2</sub>, and combustion at 450 °C for 3 min in O<sub>2</sub> (removal of the most refractory OC). Then, EC is isolated by heating the remaining carbon at 650 °C for 5 min in O<sub>2</sub>. Details can be found in Zenker et al. (2017) and Ni et al. (2018).

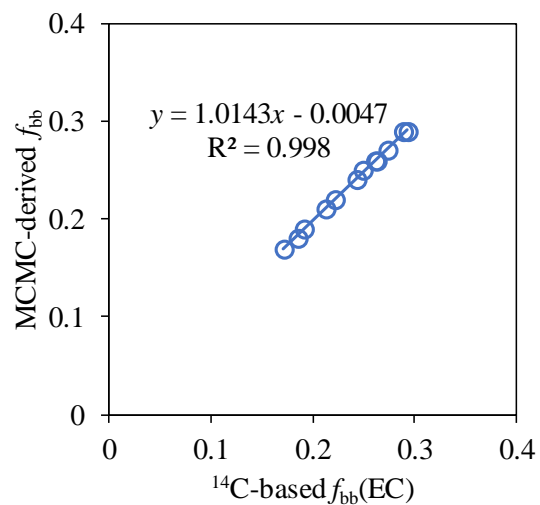


**Figure S3.** Comparison between the MCMC-derived fraction of biomass burning EC ( $f_{bb}$  derived from MCMC; median) and that obtained from radiocarbon data ( $^{14}\text{C}$ -based  $f_{bb}(\text{EC})$ ; mean).

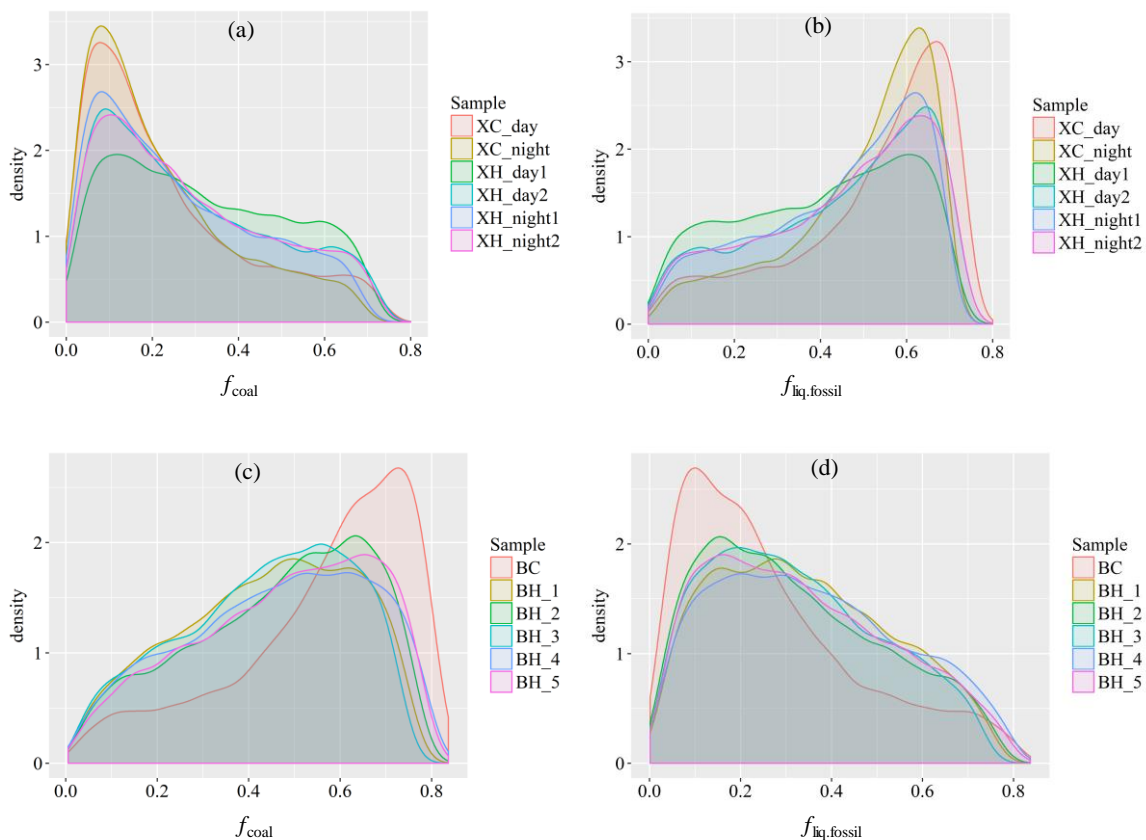


**Figure S4.** Probability density functions (PDFs) of the relative source contribution of coal combustion ( $f_{\text{coal}}$ ) in Xi'an **(a)** and Beijing **(c)**. PDFs of the relative source contribution of liquid fossil fuel combustion ( $f_{\text{liq.fossil}}$ ) in Xi'an **(b)** and Beijing **(d)**.  $f_{\text{coal}}$  and  $f_{\text{liq.fossil}}$  are constrained by combining radiocarbon and  $\delta^{13}\text{C}$  measurements of EC, calculated using the Bayesian Markov chain Monte Carlo approach. For details, see Sect. 2.4.

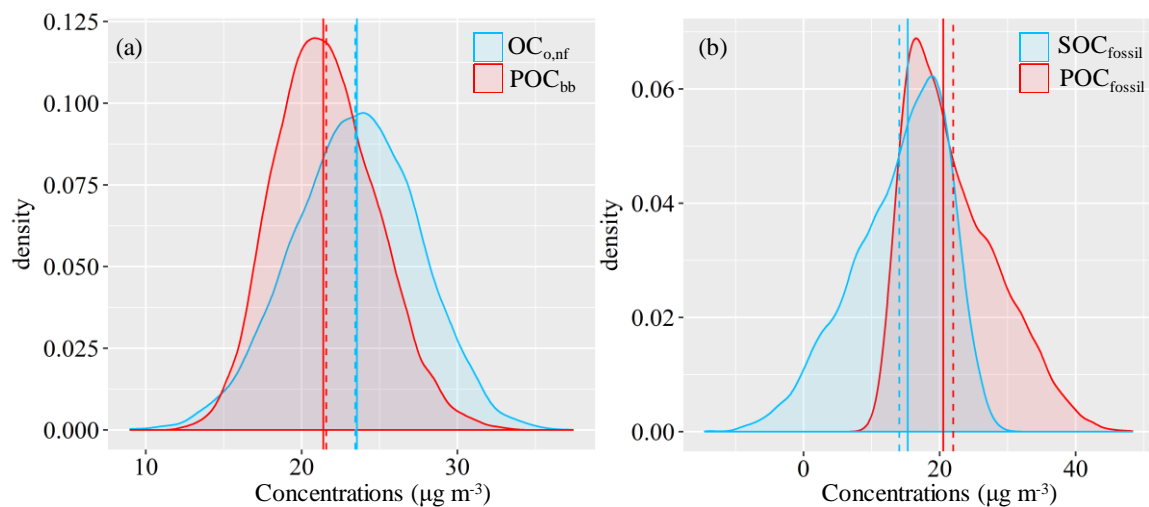


**Figure S5.** (a) Example probability density functions (PDFs) of concentrations of  $\text{OC}_{\text{o,nf}}$  (light blue) and  $\text{POC}_{\text{bb}}$  (red) for sample XH\_day2. (b) PDFs of concentrations of  $\text{SOC}_{\text{fossil}}$  (light blue) and  $\text{POC}_{\text{fossil}}$  (red) for the same sample. Their concentrations are estimated from  $^{14}\text{C}$ -apportioned OC and EC using the EC tracer method (Sect. 2.4). The mean and median are indicated by the dashed and solid vertical lines, respectively.

**Table S1.** Details of sampling information and selected samples for radiocarbon measurements.

City	Descriptions	Selected samples for $^{14}\text{C}$ analysis			RH*	Temperature ( $^{\circ}\text{C}$ )	Wind speed ( $\text{m s}^{-1}$ )
		Sample name	Note	Sampling Date/Time			
Xi'an	PM <sub>2.5</sub> samples were collected on the rooftop (~10 m) of a two-floor building located at the Institute of Earth Environment, Chinese Academy of Sciences (34.2° N, 108.9° E). This site is a typical urban background site surrounded by residential and education areas.	XH_day1	Haze/daytime	2017.1.1/Daytime 2017.1.2/Daytime	69 (56~91)	4.2 (-1.5~8.3)	1.0 (0.0~2.6)
		XH_night1	Haze/nighttime	2017.1.1/Nighttime 2017.1.2/Nighttime	88 (68~96)	0.3 (-2.6~3.5)	1.3 (0.2~2.5)
		XH_day2	Haze/daytime	2017.1.3/Daytime 2017.1.4/Daytime	78 (64~96)	4.4 (-2.6~7.2)	1.0 (0.0~2.3)
		XH_night2	Haze/nighttime	2017.1.3/Nighttime 2017.1.4/Nighttime	93 (84~97)	0.8 (-0.6~4.1)	0.6 (0.0~1.2)
		XC_day	Clean/daytime	2017.1.7/Daytime 2017.1.8/Daytime	60 (40~93)	4.4 (-4.2~8.0)	1.6 (0.4~2.6)
		XC_night	Clean/nighttime	2017.1.7/Nighttime 2017.1.8/Nighttime	85 (75~93)	-0.9 (-3.6~1.0)	1.0 (0.0~1.8)
Beijing	24 h integrated PM <sub>2.5</sub> samples were collected on the roof of a five-story building (~20 m) at the National Centre for Nanoscience (39.99° N, 116.32° E). The sampling site is close to the fourth ring of Beijing, and surrounded by residential, commercial and traffic areas.	BH_1	Haze	2016.12.11	59 (47~72)	0.7 (-1.7~2.1)	1.1 (0.4~1.7)
		BH_2	Haze	2016.12.17	66 (38~91)	-0.7 (-5.7~5.8)	0.8 (0.0~1.9)
		BH_3	Haze	2016.12.20	78 (55~88)	0.7 (-1.2~3.7)	1.1 (0.3~2.2)
		BH_4	Haze	2017.1.1 2017.1.2	59 (25~89)	0.0 (-5.7~8.2)	1.4 (0.3~3.1)
		BH_5	Haze	2017.1.4	73 (34~90)	1.1 (-3.0~7.3)	1.1 (0.0~1.7)
		BC	Clean	2016.12.26 2017.1.8	33 (22~48)	0.5 (-4.9~8.0)	1.8 (0.3~3.3)

\*The meteorological data (mean; minimum-maximum) is obtained from the Meteorological Institute of Shaanxi Province, Xi'an, China.



**Table S2.** Fraction modern ( $F^{14}C$ ) of elemental carbon (EC), organic carbon (OC) ( $F^{14}C_{(EC)}$  and  $F^{14}C_{(OC)}$ , respectively), and stable carbon isotopic compositions ( $\delta^{13}C$ , ‰) of EC ( $\delta^{13}C_{EC}$ ).

Sample name	Note	Sampling Date/Time	$F^{14}C_{(EC)}^a$	$F^{14}C_{(OC)}^a$	$\delta^{13}C_{EC}^a$
XH_day1	Haze/daytime	2017.1.1/Daytime 2017.1.2/Daytime	$0.301 \pm 0.007$	$0.594 \pm 0.004$	$-24.38 \pm 0.02$
XH_night1	Haze/nighttime	2017.1.1/Nighttime 2017.1.2/Nighttime	$0.321 \pm 0.014$	$0.608 \pm 0.005$	$-25.02 \pm 0.01$
XH_day2	Haze/daytime	2017.1.3/Daytime 2017.1.4/Daytime	$0.287 \pm 0.009$	$0.605 \pm 0.004$	$-24.92 \pm 0.04$
XH_night2	Haze/nighttime	2017.1.3/Nighttime 2017.1.4/Nighttime	$0.288 \pm 0.010$	$0.603 \pm 0.004$	$-24.87 \pm 0.03$
XC_day	Clean/daytime	2017.1.7/Daytime 2017.1.8/Daytime	$0.273 \pm 0.005$	$0.550 \pm 0.004$	$-25.53 \pm 0.02$
XC_night	Clean/nighttime	2017.1.7/Nighttime 2017.1.8/Nighttime	$0.317 \pm 0.004$	$0.590 \pm 0.004$	$-25.63 \pm 0.03$
BH_1	Haze	2016.12.11	$0.243 \pm 0.005$	$0.383 \pm 0.005$	$-24.43 \pm 0.03$
BH_2	Haze	2016.12.17	$0.233 \pm 0.005$	$0.368 \pm 0.005$	$-24.09 \pm 0.04$
BH_3	Haze	2016.12.20	$0.266 \pm 0.005$	$0.390 \pm 0.004$	$-24.38 \pm 0.02$
BH_4	Haze	2017.1.1 2017.1.2	$0.203 \pm 0.005$	$0.333 \pm 0.004$	$-24.29 \pm 0.02$
BH_5	Haze	2017.1.4	$0.211 \pm 0.003$	$0.334 \pm 0.003$	$-24.15 \pm 0.01$
BC	Clean	2016.12.26 2017.1.8	$0.188 \pm 0.006$	$0.403 \pm 0.005$	$-23.41 \pm 0.01$

<sup>a</sup> Values are given in average  $\pm$  measurement uncertainty.

**Table S3.** Fraction of non-fossil carbon in EC and OC ( $f_{bb}(EC)$ ,  $f_{nf}(OC)$ ), fraction of fossil carbon in EC and OC ( $f_{fossil}(EC)$ ,  $f_{fossil}(OC)$ ), concentrations ( $\mu\text{g m}^{-3}$ ) of EC and OC from non-fossil sources ( $EC_{bb}$  and  $OC_{nf}$ ) and fossil sources ( $EC_{fossil}$  and  $OC_{fossil}$ ) during haze and clean periods in Xi'an and Beijing during December 2016 and January 2017. Details of samples are shown in Table S1.

Sample name	$f_{bb}(EC)$	$f_{fossil}(EC)$	$f_{nf}(OC)$	$f_{fossil}(OC)$	$EC_{bb}$	$EC_{fossil}$	$OC_{nf}$	$OC_{fossil}$
XH_day1	$0.274 \pm 0.008$	$0.726 \pm 0.008$	$0.545 \pm 0.011$	$0.455 \pm 0.011$	$3.48 \pm 0.36$	$9.24 \pm 0.91$	$28.49 \pm 1.53$	$23.74 \pm 1.31$
XH_night1	$0.292 \pm 0.014$	$0.708 \pm 0.014$	$0.558 \pm 0.011$	$0.442 \pm 0.011$	$4.23 \pm 0.47$	$10.24 \pm 1.05$	$31.23 \pm 1.70$	$24.77 \pm 1.40$
XH_day2	$0.261 \pm 0.010$	$0.739 \pm 0.010$	$0.555 \pm 0.011$	$0.445 \pm 0.011$	$5.37 \pm 0.58$	$15.22 \pm 1.55$	$45.04 \pm 2.41$	$36.08 \pm 2.02$
XH_night2	$0.262 \pm 0.010$	$0.738 \pm 0.010$	$0.553 \pm 0.011$	$0.447 \pm 0.011$	$6.37 \pm 0.69$	$17.96 \pm 1.82$	$48.97 \pm 2.62$	$39.55 \pm 2.22$
XC_day	$0.248 \pm 0.006$	$0.752 \pm 0.006$	$0.505 \pm 0.010$	$0.495 \pm 0.010$	$2.17 \pm 0.23$	$6.56 \pm 0.66$	$12.61 \pm 0.68$	$12.37 \pm 0.66$
XC_night	$0.288 \pm 0.006$	$0.712 \pm 0.006$	$0.542 \pm 0.011$	$0.458 \pm 0.011$	$1.76 \pm 0.18$	$4.33 \pm 0.44$	$9.31 \pm 0.50$	$7.88 \pm 0.44$
BH_1	$0.221 \pm 0.006$	$0.779 \pm 0.006$	$0.352 \pm 0.008$	$0.648 \pm 0.008$	$3.04 \pm 0.32$	$10.71 \pm 1.08$	$15.02 \pm 0.83$	$27.66 \pm 1.44$
BH_2	$0.212 \pm 0.006$	$0.788 \pm 0.006$	$0.337 \pm 0.008$	$0.663 \pm 0.008$	$2.80 \pm 0.29$	$10.44 \pm 1.04$	$13.13 \pm 0.71$	$25.81 \pm 1.31$
BH_3	$0.242 \pm 0.006$	$0.758 \pm 0.006$	$0.358 \pm 0.008$	$0.642 \pm 0.008$	$3.97 \pm 0.41$	$12.42 \pm 1.25$	$18.62 \pm 1.01$	$33.43 \pm 1.72$
BH_4	$0.185 \pm 0.006$	$0.815 \pm 0.006$	$0.306 \pm 0.007$	$0.694 \pm 0.007$	$2.24 \pm 0.23$	$9.86 \pm 0.97$	$11.35 \pm 0.62$	$25.77 \pm 1.29$
BH_5	$0.191 \pm 0.004$	$0.809 \pm 0.004$	$0.306 \pm 0.007$	$0.694 \pm 0.007$	$2.31 \pm 0.24$	$9.74 \pm 0.97$	$12.23 \pm 0.67$	$27.68 \pm 1.42$
BC	$0.171 \pm 0.006$	$0.829 \pm 0.006$	$0.370 \pm 0.008$	$0.630 \pm 0.008$	$0.27 \pm 0.03$	$1.33 \pm 0.13$	$2.54 \pm 0.14$	$4.34 \pm 0.23$

**Table S4.** Concentrations ( $\mu\text{g m}^{-3}$ ) of primary OC from biomass burning ( $\text{POC}_{\text{bb}}$ ), primary OC from fossil sources, OC from non-fossil sources excluding primary biomass burning ( $\text{OC}_{\text{o,nf}}$ ), secondary OC from fossil sources ( $\text{SOC}_{\text{fossil}}$ ) and total SOC (i.e., approximately the sum of  $\text{OC}_{\text{o,nf}}$  and  $\text{SOC}_{\text{fossil}}$ ) during haze and clean periods in Xi'an and Beijing during December 2016 and January 2017 (median and interquartile range). Details of samples are shown in Table S1.

Sample name	$\text{POC}_{\text{bb}}$	$\text{POC}_{\text{fossil}}$	$\text{OC}_{\text{o,nf}}$	$\text{SOC}_{\text{fossil}}$	SOC	$f_{\text{fossil}}(\text{SOC})$
XH_day1	13.82 (12.50–15.26)	13.38 (10.61–16.88)	14.58 (12.83–16.25)	10.34 (6.71–13.16)	24.56 (20.53–28.25)	0.41 (0.32–0.47)
XH_night1	16.80 (15.14–18.58)	13.80 (11.24–17.61)	14.40 (12.27–16.41)	10.82 (7.04–13.61)	24.81 (20.35–28.80)	0.43 (0.33–0.49)
XH_day2	21.43 (19.28–23.68)	20.50 (16.60–26.58)	23.54 (20.75–26.20)	15.41 (9.35–19.52)	38.29 (31.42–44.04)	0.40 (0.29–0.45)
XH_night2	25.40 (22.88–28.07)	24.32 (19.66–30.96)	23.51 (20.34–26.62)	15.06 (8.37–19.94)	37.85 (30.55–44.63)	0.39 (0.27–0.46)
XC_day	8.64 (7.77–9.54)	8.21 (6.82–10.63)	3.98 (2.95–4.94)	4.07 (1.73–5.59)	7.76 (5.18–9.89)	0.52 (0.36–0.60)
XC_night	6.99 (6.30–7.72)	5.37 4.46–6.85	2.32 1.51–3.07	2.47 1.00–3.43	4.57 2.83–6.07	0.53 0.38–0.64
BH_1	12.15 (10.90–13.44)	18.32 (14.82–21.65)	2.87 (1.47–4.27)	9.44 (5.86–12.99)	12.33 98.13–16.41)	0.76 (0.67–0.86)
BH_2	11.17 (10.04–12.34)	18.36 (14.89–21.44)	1.98 (0.65–3.17)	7.56 (4.26–11.04)	9.59 (5.67–13.45)	0.80 (0.68–0.91)
BH_3	15.82 (14.21–17.56)	21.21 (17.18–25.02)	2.77 (0.95–4.50)	12.24 (8.16–16.36)	15.01 (10.19–19.75)	0.81 (0.72–0.92)
BH_4	8.88 (8.00–9.84)	16.95 (13.83–19.94)	2.45 (1.41–3.44)	8.79 (5.70–12.06)	11.30 (7.71–14.83)	0.78 (0.70–0.86)
BH_5	9.17 (8.25–10.17)	16.94 (13.73–19.86)	3.00 (1.96–4.07)	10.79 (7.65–14.08)	13.82 (10.26–17.53)	0.78 (0.71–0.85)
BC	1.09 (0.98–1.21)	2.55 (2.15–2.90)	1.44 (1.30–1.59)	1.80 (1.42–2.22)	3.26 (2.79–3.76)	0.55 (0.50–0.60)

**Table S5.** Fractional contribution of different incomplete combustion sources to EC in different seasons ( $f_{bb}$ ,  $f_{liq.fossil}$  and  $f_{coal}$ ; median and interquartile range ), and EC concentrations ( $\mu\text{g m}^{-3}$ ) from biomass burning ( $EC_{bb}$ ), coal combustion ( $EC_{coal}$ ) and liquid fossil fuel combustion ( $EC_{liq.fossil}$ ) (median and interquartile range). Details of samples are shown in Table S1.

City	Sample Name	Note	$f_{bb}$	$f_{liq.fossil}$	$f_{coal}$	$EC_{bb}$	$EC_{liq.fossil}$	$EC_{coal}$
Xi'an	XH_day1	Haze1/daytime	0.27 (0.27–0.28)	0.44 (0.26–0.58)	0.29 (0.14–0.47)	3.48 (3.24–3.73)	5.49 (3.10–7.30)	3.66 (1.82–5.98)
	XH_night1	Haze1/nighttime	0.29 (0.29–0.30)	0.47 (0.30–0.59)	0.23 (0.12–0.41)	4.23 (3.93–4.54)	6.75 (4.28–8.45)	3.29 (1.69–5.87)
	XH_day2	Haze2/daytime	0.29 (0.29–0.30)	0.47 (0.30–0.59)	0.23 (0.12–0.41)	5.38 (4.99–5.78)	10.04 (6.15–12.60)	4.94 (2.44–8.94)
	XH_night2	Haze2/nighttime	0.26 (0.26–0.27)	0.49 (0.30–0.62)	0.25 (0.12–0.44)	6.39 (5.94–6.85)	11.85 (7.40–14.93)	5.88 (2.91–10.35)
	XC_day	Clean/daytime	0.25 (0.24–0.26)	0.57 (0.40–0.66)	0.18 (0.09–0.35)	2.17 (2.01–2.32)	4.73 (3.23–5.68)	1.69 (0.83–3.24)
	XC_night	Clean/nighttime	0.29 (0.28–0.30)	0.54 (0.38–0.62)	0.17 (0.09–0.33)	1.76 (1.63–1.89)	3.17 (2.21–3.76)	1.07 (0.53–2.05)
Beijing	BH_1	Haze1	0.22 (0.21–0.23)	0.32 (0.18–0.49)	0.46 (0.29–0.60)	3.05 (2.83–3.28)	4.38 (2.49–6.68)	6.18 (3.90–8.18)
	BH_2	Haze2	0.21 (0.21–0.22)	0.29 (0.16–0.46)	0.50 (0.33–0.62)	2.80 (2.59–3.02)	3.89 (2.15–6.13)	6.42 (4.20–8.15)
	BH_3	Haze3	0.24 (0.23–0.25)	0.31 (0.18–0.47)	0.45 (0.29–0.58)	3.98 (3.69–4.28)	5.14 (2.99–7.79)	7.17 (4.52–9.38)
	BH_4	Haze4	0.19 (0.18–0.19)	0.33 (0.18–0.50)	0.49 (0.31–0.63)	2.24 (2.07–2.40)	3.90 (2.21–6.00)	5.80 (3.75–7.53)
	BH_5	Haze5	0.19 (0.19–0.20)	0.31 (0.17–0.48)	0.50 (0.33–0.63)	2.31 (2.13–2.48)	3.75 (2.09–5.87)	5.86 (3.73–7.55)
	BC	Clean	0.17 (0.17–0.18)	0.22 (0.12–0.37)	0.61 (0.46–0.71)	0.27 (0.25–0.30)	0.35 (0.18–0.59)	0.96 (0.72–1.14)

**Table S6.** Fractional contribution of different incomplete combustion sources to EC (median and interquartile range).

	Biomass burning	Coal combustion	Liquid fossil fuel combustion (i.e., vehicle emissions)
Xi'an haze day	0.27 (0.26–0.27)	0.26 (0.13–0.44)	0.47 (0.29–0.60)
Xi'an haze night	0.28 (0.27–0.28)	0.23 (0.12–0.41)	0.49 (0.31–0.61)
Xi'an clean day	0.25 (0.24–0.26)	0.18 (0.09–0.33)	0.57 (0.42–0.66)
Xi'an clean night	0.29 (0.28–0.30)	0.18 (0.09–0.34)	0.53 (0.37–0.62)
Beijing haze	0.21 (0.20–0.22)	0.48 (0.31–0.61)	0.31 (0.18–0.48)
Beijing clean	0.17 (0.17–0.18)	0.61 (0.45–0.71)	0.22 (0.12–0.38)

## References

Dusek, U., Monaco, M., Prokopiou, M., Gongriep, F., Hitzenberger, R., Meijer, H. A. J., and Röckmann, T.: Evaluation of a two-step thermal method for separating organic and elemental carbon for radiocarbon analysis, *Atmos. Meas. Tech.*, 7, 1943–1955, <https://doi.org/10.5194/amt-7-1943-2014>, 2014.

Ni, H., Huang, R.-J., Cao, J., Liu, W., Zhang, T., Wang, M., Meijer, H. A. J., and Dusek, U.: Source apportionment of carbonaceous aerosols in Xi'an, China: insights from a full year of measurements of radiocarbon and the stable isotope  $^{13}\text{C}$ , *Atmos. Chem. Phys.*, 18, 16363–16383, <https://doi.org/10.5194/acp-18-16363-2018>, 2018.

Zenker, K., Vonwiller, M., Szidat, S., Calzolari, G., Giannoni, M., Bernardoni, V., Jedynska, A. D., Henzing, B., Meijer, H. A., and Dusek, U.: Evaluation and Inter-comparison of oxygen-based OC-EC separation methods for radiocarbon analysis of ambient aerosol particle samples, *Atmosphere*, 8, 226, <https://doi.org/10.3390/atmos8110226>, 2017.

Zhang, Y. L., Li, J., Zhang, G., Zotter, P., Huang, R.-J., Tang, J.-H., Wacker, L., Prévôt, A. S. H., and Szidat, S.: Radiocarbon-based source apportionment of carbonaceous aerosols at a regional background site on Hainan Island, South China, *Environ. Sci. Technol.*, 48, 2651–2659, <https://doi.org/10.1021/es4050852>, 2014.

Zhang, Y. L., Huang, R. J., El Haddad, I., Ho, K. F., Cao, J. J., Han, Y., Zotter, P., Bozzetti, C., Daellenbach, K. R., Canonaco, F., Slowik, J. G., Salazar, G., Schwikowski, M., Schnelle-Kreis, J., Abbazade, G., Zimmermann, R., Baltensperger, U., Prévôt, A. S. H., and Szidat, S.: Fossil vs. non-fossil sources of fine carbonaceous aerosols in four Chinese cities during the extreme winter haze episode of 2013, *Atmos. Chem. Phys.*, 15, 1299–1312, <https://doi.org/10.5194/acp-15-1299-2015>, 2015.